Few Body Syst (2007) 41: 117–140
DOI 10.1007/s00601-007-0193-3
Printed in The Netherlands

Few-Body Systems

Local three-nucleon interaction from chiral effective field theory

P. Navrátil*

Lawrence Livermore National Laboratory, Livermore, CA, USA

Received 3 August 2007; Accepted 18 October 2007; Published online 30 November 2007

Abstract The three-nucleon (*NNN*) interaction derived within the chiral effective field theory at the next-to-next-to-leading order (N^2LO) is regulated with a function depending on the magnitude of the momentum transfer. The regulated *NNN* interaction is then local in the coordinate space, which is advantageous for some many-body techniques. Matrix elements of the local chiral *NNN* interaction are evaluated in a three-nucleon basis. Using the *ab initio* no-core shell model (NCSM) the *NNN* matrix elements are employed in ^{3}H and ^{4}He bound-state calculations.

1 Introduction

Interactions among nucleons are governed by quantum chromodynamics (QCD). In the low-energy regime relevant to nuclear structure, QCD is non-perturbative, and, therefore, hard to solve. Thus, theory has been forced to resort to models for the interaction, which have limited physical basis. New theoretical developments, however, allow us to connect QCD with low-energy nuclear physics. The chiral effective field theory (χEFT) [1] provides a promising bridge. Beginning with the pionic or the nucleon-pion system [2], one works consistently with systems of increasing nucleon number [3–5]. One makes use of spontaneous breaking of chiral symmetry to systematically expand the strong interaction in terms of a generic small momentum and takes the explicit breaking of chiral symmetry into account by expanding in the pion mass. Thereby, the *NN* interaction, the *NNN* interaction and also πN scattering are related to each other. At the same time, the pion mass dependence of the interaction is known, which will enable a connection to lattice QCD calcula-

E-mail address: navratil1@llnl.gov

Correspondence: P. Navrátil, Lawrence Livermore National Laboratory, L-414, P.O. Box 808, Livermore, CA 94551, USA

tions in the future [6]. Nuclear interactions are non-perturbative, because diagrams with purely nucleonic intermediate states are enhanced [1]. Therefore, the chiral perturbation expansion is performed for the potential (note, however, the discussion in [7–9] that points out some potential inconsistencies of this approach). Solving the Schrödinger equation for this potential then automatically sums diagrams with purely nucleonic intermediate states to all orders. The χEFT predicts, along with the *NN* interaction at the leading order, an *NNN* interaction at the 3rd order (next-to-next-to-leading order or N^{2}LO) [1, 10, 11], and even an *NNNN* interaction at the fourth order (N^{3}LO) [12]. The details of QCD dynamics are contained in parameters, low-energy constants (LECs), not fixed by the symmetry. These parameters can be constrained by experiment. At present, high-quality *NN* potentials have been determined at order N^{3}LO [13]. A crucial feature of χEFT is the consistency between the *NN*, *NNN* and *NNNN* parts. As a consequence, at N^{2}LO and N^{3}LO, except for two LECs, assigned to two *NNN* diagrams, the potential is fully constrained by the parameters defining the *NN* interaction.

It is of great interest and also a challenge to apply the chiral interactions in nuclear structure and nuclear reaction calculations. In a recent work [14], the presently available *NN* potential at N^{3}LO [13] and the *NNN* interaction at N^{2}LO [10, 11] have been applied to the calculation of various properties of *s*- and *p*-shell nuclei, using the *ab initio* no-core shell model (NCSM) [15, 16], up to now the only approach able to handle the nonlocal χEFT *NN* potentials for systems beyond $A = 4$. In that study, a preferred choice of the two *NNN* LECs, c_D and c_E, was found and the fundamental importance of the χEFT *NNN* interaction was demonstrated for reproducing the structure of mid-*p*-shell nuclei. In a subsequent study, the same Hamiltonian was used to calculate microscopically the photo-absorption cross section of ^{4}He [17].

The approach of [14] differs in two aspects from the first NCSM application of the χEFT *NN* + *NNN* interactions in [18], which presents a detailed investigation of ^{7}Li. First, a regulator depending on the momentum transfer in the *NNN* terms was introduced which results in a local χEFT *NNN* interaction. Second, the ^{4}He binding energy was not used exclusively as the second constraint on the c_D and c_E LECs.

A local *NNN* interaction is advantageous for some few- and many-body approaches because it is simpler to use. At the same time, it is known that details of the *NNN* interaction are important for nuclear structure applications. For example, the Urbana IX [19] and the Tucson-Melbourne [20–22] *NNN* interactions perform differently in mid-*p*-shell nuclei [23, 24, 16] although their differences appear to be minor. In the Green's function Monte Carlo (GFMC) calculations with the AV18 *NN* potential [25], the best results for *p*-shell nuclei up to $A = 10$ are found using the Illinois *NNN* interaction that augments the Urbana IX by a two-pion term from the Tucson-Melbourne *NNN* interaction and by three-pion terms that in the χEFT appear beyond the N^{3}LO [26, 27]. Contrary to the Illinois *NNN* interaction, the χEFT *NNN* interaction features the above-mentioned consistency with the accompanying *NN* interaction. Still, interestingly, we found that the nonlocal χEFT *NNN* interaction used in [18] and the local χEFT *NNN* interaction employed in [14] differ to some extent in their description of mid-*p*-shell nuclei with the latter giving

results in a better agreement with experiment. Therefore, it is important to pay attention to the details of the *NNN* interaction and test different possibilities.

It is the purpose of this paper to elaborate on the details of the local χEFT *NNN* interaction used in [14, 17] and present its matrix elements in the three-nucleon basis. Technical details of dealing with *NNN* interactions were investigated in many papers [28–34]. A new feature in the present work is the use of χEFT contact interactions and a focus on the application within the *ab initio* NCSM. In particular, we demonstrate the binding-energy convergence of the three-nucleon and four-nucleon systems with the χEFT $NN + NNN$ interactions using the *ab initio* NCSM. In Sect. 2, the local χEFT *NNN* interaction is discussed and compared to the nonlocal version of [11]. Its three-nucleon matrix elements are given term by term. In Sect. 3, the ^{3}H and ^{4}He binding energy and radius calculation results using the N^{3}LO χEFT *NN* interaction of [13] and the local χEFT *NNN* interaction are given. Conclusions are drawn in Sect. 4.

2 Local χEFT *NNN* interaction at N^{2}LO

The *NNN* interaction appearing at the third order (N^{2}LO) of the χEFT comprises of three parts: (i) The two-pion exchange, (ii) the one-pion exchange plus contact, and (iii) the three-nucleon contact. In this section, we discuss all the parts in detail and present the three-nucleon matrix elements of all the terms. For the two parts that contain the contact interactions, we also discuss in detail the impact of different regularization schemes.

2.1 Three-nucleon coordinates

We use the following definitions of the Jacobi coordinates

$$\boldsymbol{\xi}_1 = \frac{1}{\sqrt{2}}(\boldsymbol{r}_1 - \boldsymbol{r}_2), \tag{1}$$

$$\boldsymbol{\xi}_2 = \sqrt{\frac{2}{3}}\left(\frac{1}{2}(\boldsymbol{r}_1 + \boldsymbol{r}_2) - \boldsymbol{r}_3\right), \tag{2}$$

and associated momenta

$$\boldsymbol{\pi}_1 = \frac{1}{\sqrt{2}}(\boldsymbol{p}_1 - \boldsymbol{p}_2), \tag{3}$$

$$\boldsymbol{\pi}_2 = \sqrt{\frac{2}{3}}\left(\frac{1}{2}(\boldsymbol{p}_1 + \boldsymbol{p}_2) - \boldsymbol{p}_3\right). \tag{4}$$

We also define the momenta transferred by nucleon 2 and nucleon 3,

$$\boldsymbol{Q} = \boldsymbol{p}_2' - \boldsymbol{p}_2 = -\frac{1}{\sqrt{2}}(\boldsymbol{\pi}_1' - \boldsymbol{\pi}_1) + \frac{1}{\sqrt{6}}(\boldsymbol{\pi}_2' - \boldsymbol{\pi}_2), \tag{5}$$

$$\boldsymbol{Q}' = \boldsymbol{p}_3' - \boldsymbol{p}_3 = -\sqrt{\frac{2}{3}}(\boldsymbol{\pi}_2' - \boldsymbol{\pi}_2), \tag{6}$$

where the primed coordinates refer to the initial momentum and the unprimed to the final momentum of the nucleon.

2.2 General structure of three-nucleon interaction and its matrix element

The *NNN* interaction is symmetric under permutation of the three nucleon indexes. It can be written as a sum of three pieces related by particle permutations,

$$W = W_1 + W_2 + W_3. \tag{7}$$

To obtain its matrix element in an antisymmetrized three-nucleon basis we need to consider just a single term, e.g., W_1. In this paper, we use the basis of harmonic oscillator (HO) wave functions. However, most of the expressions have general validity. Following the notation of [35], a general matrix element can be written as

$$\begin{aligned}\langle NiJT|W|N'i'JT\rangle &= 3\langle NiJT|W_1|N'i'JT\rangle \\ &= 3\sum\langle nlsjt,\mathcal{NLJ}||NiJT\rangle\langle n'l's'j't',\mathcal{N}'\mathcal{L}'\mathcal{J}'||N'i'JT\rangle \\ &\quad\times\langle(nlsjt,\mathcal{NLJ})JT|W_1|(n'l's'j't',\mathcal{N}'\mathcal{L}'\mathcal{J}')JT\rangle,\end{aligned} \tag{8}$$

where $|NiJT\rangle$ is an antisymmetrized three-nucleon state with $N = 2n + l + 2\mathcal{N} + \mathcal{L}$, i an additional quantum number, and J and T are the total angular momentum and total isospin, respectively. The parity of the state is $(-1)^N$. The state $|(nlsjt,\mathcal{NLJ})JT\rangle$ is a product of the HO wave functions $\langle\boldsymbol{\xi}_1|nl\rangle$ and $\langle\boldsymbol{\xi}_2|\mathcal{NL}\rangle$ associated with the coordinates (1) and (2), respectively. This state is antisymmetrized only with respect to the exchange of nucleons 1 and 2, i.e., $(-1)^{l+s+t} = -1$. The coefficient of fractional parentage $\langle nlsjt,\mathcal{NLJ}||NiJT\rangle$ is calculated according to [35].

2.3 N^{2}LO three-nucleon interaction contact term

We start our discussion with the most trivial part of the χEFT N^{2}LO *NNN* interaction, the three-nucleon contact term

$$\begin{aligned}W_1^{\text{cont}} &= E\,\boldsymbol{\tau}_2\cdot\boldsymbol{\tau}_3\,\delta(\boldsymbol{r}_1-\boldsymbol{r}_2)\,\delta(\boldsymbol{r}_3-\boldsymbol{r}_1) \\ &= E\,\boldsymbol{\tau}_2\cdot\boldsymbol{\tau}_3\,\frac{1}{(2\pi)^6}\frac{1}{(\sqrt{3})^3}\int d\boldsymbol{\pi}_1\,d\boldsymbol{\pi}_2\,d\boldsymbol{\pi}'_1\,d\boldsymbol{\pi}'_2\,|\boldsymbol{\pi}_1\boldsymbol{\pi}_2\rangle\langle\boldsymbol{\pi}'_1\boldsymbol{\pi}'_2|,\end{aligned} \tag{9}$$

with $E = c_E/F_\pi^4\Lambda_\chi$, where Λ_χ is the chiral symmetry breaking scale of the order of the ρ meson mass and $F_\pi = 92.4\,\text{MeV}$ is the weak pion decay constant. The c_E is a

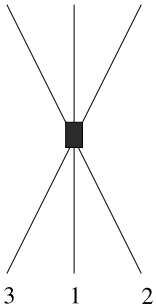

Fig. 1 Contact interaction *NNN* term of the N^{2}LO χEFT

low-energy constant (LEC) from the chiral Lagrangian of order one. The corresponding diagram is shown in Fig. 1. This term was regulated in [11] by a regulator dependent on the sum of Jacobi momenta squared,

$$W_1^{\text{cont,ENGKMW}} = E\,\boldsymbol{\tau}_2\cdot\boldsymbol{\tau}_3\,\frac{1}{(2\pi)^6}\frac{1}{(\sqrt{3})^3}\int d\boldsymbol{\pi}_1\,d\boldsymbol{\pi}_2\,d\boldsymbol{\pi}_1'\,d\boldsymbol{\pi}_2'|\boldsymbol{\pi}_1\boldsymbol{\pi}_2\rangle \times F\left(\frac{1}{2}(\pi_1^2+\pi_2^2);\Lambda\right)F\left(\frac{1}{2}(\pi_1'^2+\pi_2'^2);\Lambda\right)\langle\boldsymbol{\pi}_1'\boldsymbol{\pi}_2'|, \quad (10)$$

with the regulator function

$$F(q^2;\Lambda) = \exp[-q^4/\Lambda^4] \quad (11)$$

with the limit $F(q^2;\Lambda\to\infty)=1$. This was in particular convenient as the calculations were performed in momentum space. In Eq. (10), the abbreviation ENGKMW stands for the initial letters of the names of authors of [11]. We note that an identical regulator function (11) was chosen in [13]. We use this form in our numerical calculations presented in Sect. 3. However, until then we keep our discussion general and do not restrict ourselves to a particular choice of the regulator function. It should be noted that a smoother regulator of the form $F(q^2;\Lambda)=\exp[-q^2/\Lambda^2]$ would have lead to a simplified algebra. The fourth power of the momentum in Eq. (11) was chosen in [11] so that the regulator generates powers which are beyond the third order at which the calculations are conducted.

Alternatively to Eq. (10), let us consider a regulator dependent on momentum transfer,

$$\begin{aligned} W_1^{\text{cont,Q}} &= E\,\boldsymbol{\tau}_2\cdot\boldsymbol{\tau}_3\,\frac{1}{(2\pi)^6}\frac{1}{(\sqrt{3})^3}\int d\boldsymbol{\pi}_1\,d\boldsymbol{\pi}_2\,d\boldsymbol{\pi}_1'\,d\boldsymbol{\pi}_2'\,|\boldsymbol{\pi}_1\boldsymbol{\pi}_2\rangle \\ &\quad\times F(\boldsymbol{Q}^2;\Lambda)F(\boldsymbol{Q}'^2;\Lambda)\langle\boldsymbol{\pi}_1'\boldsymbol{\pi}_2'| \\ &= E\,\boldsymbol{\tau}_2\cdot\boldsymbol{\tau}_3\int d\boldsymbol{\xi}_1\,d\boldsymbol{\xi}_2|\boldsymbol{\xi}_1\boldsymbol{\xi}_2\rangle Z_0(\sqrt{2}\xi_1;\Lambda) \\ &\quad\times Z_0\left(\left|\frac{1}{\sqrt{2}}\,\boldsymbol{\xi}_1+\sqrt{\frac{3}{2}}\boldsymbol{\xi}_2\right|;\Lambda\right)\langle\boldsymbol{\xi}_1\boldsymbol{\xi}_2|, \end{aligned} \quad (12)$$

where we introduced the function

$$Z_0(r;\Lambda) = \frac{1}{2\pi^2}\int dq\,q^2 j_0(qr)F(q^2;\Lambda). \quad (13)$$

This results in an interaction local in coordinate space because of the dependence of the regulator function on differences of initial and final Jacobi momenta. An interaction local in coordinate space may be more convenient for some methods. In fact, most of the *NNN* interactions used in few-body calculations, such as the Tucson-Melbourne (TM′) [21, 22], Urbana IX (UIX) [19] or Illinois 2 (IL2) [26], are local in coordinate space. Similarly, a local *NN* interaction can be derived from a momentum-space *NN* potential as was done, e.g., in the case of the Bonn potential, see [36].

The two alternatively regulated contact interactions lead to different three-nucleon matrix elements. The interaction (10) gives

$$\begin{aligned}
&\langle (nlsjt,\mathcal{NLJ})JT|W_1^{\text{cont,ENGKMW}}|(n'l's'j't',\mathcal{N}'\mathcal{L}'\mathcal{J}')JT\rangle \\
&\quad = E\frac{1}{2\sqrt{3}\pi^4}\delta_{l0}\delta_{\mathcal{L}0}\delta_{l'0}\delta_{\mathcal{L}'0}\delta_{ss'}\delta_{sj}\delta_{s'j'}\delta_{\mathcal{J}\frac{1}{2}}\delta_{\mathcal{J}'\frac{1}{2}} \\
&\qquad \times \hat{t}\hat{t}'(-1)^{t+t'+T+\frac{1}{2}}\left\{\begin{array}{ccc} t & t' & 1 \\ \frac{1}{2} & \frac{1}{2} & \frac{1}{2}\end{array}\right\}\left\{\begin{array}{ccc} t & t' & 1 \\ \frac{1}{2} & \frac{1}{2} & T\end{array}\right\} \\
&\qquad \times \int d\pi_1\, d\pi_2\, \pi_1^2\pi_2^2(-1)^{(n+\mathcal{N})}R_{n0}(\pi_1,1/b)R_{\mathcal{N}0}(\pi_2,1/b)F\left(\frac{1}{2}(\pi_1^2+\pi_2^2);\Lambda\right) \\
&\qquad \times \int d\pi_1'\, d\pi_2'\, \pi_1'^2\pi_2'^2(-1)^{(n'+\mathcal{N}')}R_{n'0}(\pi_1',1/b)R_{\mathcal{N}'0}(\pi_2',1/b)F\left(\frac{1}{2}(\pi_1'^2+\pi_2'^2);\Lambda\right),
\end{aligned} \tag{14}$$

while the interaction (12) results in the following matrix element,

$$\begin{aligned}
&\langle (nlsjt,\mathcal{NLJ})JT|W_1^{\text{cont,Q}}|(n'l's'j't',\mathcal{N}'\mathcal{L}'\mathcal{J}')JT\rangle \\
&\quad = E6\delta_{ss'}\hat{t}\hat{t}'(-1)^{t+t'+T+\frac{1}{2}}\left\{\begin{array}{ccc} t & t' & 1 \\ \frac{1}{2} & \frac{1}{2} & \frac{1}{2}\end{array}\right\}\left\{\begin{array}{ccc} t & t' & 1 \\ \frac{1}{2} & \frac{1}{2} & T\end{array}\right\} \\
&\qquad \times \hat{j}\hat{j}'\hat{\mathcal{J}}\hat{\mathcal{J}}'\hat{l}'\hat{\mathcal{L}}'(-1)^{J-\frac{1}{2}+\mathcal{J}'-\mathcal{J}+l+\mathcal{L}+s} \\
&\qquad \times \sum_X (-1)^X\hat{X}^2\left\{\begin{array}{ccc} l' & l & X \\ j & j' & s\end{array}\right\}\left\{\begin{array}{ccc} j & j' & X \\ \mathcal{J}' & \mathcal{J} & J\end{array}\right\}\left\{\begin{array}{ccc} \mathcal{J}' & \mathcal{J} & X \\ \mathcal{L} & \mathcal{L}' & \frac{1}{2}\end{array}\right\} \\
&\qquad \times (l'0X0|l0)(\mathcal{L}'0X0|\mathcal{L}0) \\
&\qquad \times \int d\xi_1\, d\xi_2\, \xi_1^2\xi_2^2 R_{nl}(\xi_1,b)R_{\mathcal{NL}}(\xi_2,b)R_{n'l'}(\xi_1,b)R_{\mathcal{N}'\mathcal{L}'}(\xi_2,b) \\
&\qquad \times Z_0(\sqrt{2}\xi_1;\Lambda)Z_{0,X}\left(\sqrt{\frac{1}{2}}\,\xi_1,\sqrt{\frac{3}{2}}\,\xi_2;\Lambda\right).
\end{aligned} \tag{15}$$

In the above expressions, we have introduced the radial HO wave functions R_{nl} with the oscillator parameter b and, further, a new function

$$Z_{0,X}(r_1,r_2;\Lambda) = \frac{1}{2\pi^2}\int dq\, q^2 j_X(qr_1)j_X(qr_2)F(q^2;\Lambda). \tag{16}$$

We also introduced the customary abbreviation $\hat{l} = \sqrt{2l+1}$. It should be noted that the two differently regulated contact interactions have different tensorial structure. One would perhaps expect that matrix elements of a local interaction will be easier to calculate. This is not the case for the discussed contact interaction. From Eq. (14) we can see that the term (10) acts only in *S*-waves. On the other hand, the local interaction (12) acts in higher partial waves as well as seen from Eq. (15). We display this schematically in Fig. 2 by breaking the symmetry of the pure contact interaction diagram (Fig. 1)

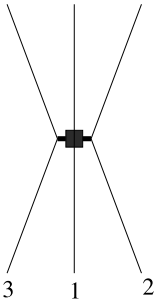

Fig. 2 Contact interaction *NNN* term of the N^{2}LO χEFT regulated by a function depending on momentum transfer

and showing the finite range of the momentum transfer regulated interaction. Using

$$F(q^2; \Lambda \to \infty) = 1,$$
$$Z_0(r, \Lambda \to \infty) = \frac{1}{4\pi r^2}\,\delta(r)$$

and

$$Z_{0,X}(r_1, r_2; \Lambda \to \infty) = \frac{1}{4\pi r_1^2}\,\delta(r_1 - r_2),$$

it is straightforward to verify that in the limit $\Lambda \to \infty$ both expressions (14) and (15) lead to the same result. For completeness, let us note that in [11] a matrix element of $\boldsymbol{\tau}_1 \cdot \boldsymbol{\tau}_2$ was calculated, i.e.,

$$\langle \boldsymbol{\tau}_1 \cdot \boldsymbol{\tau}_2 \rangle = 6\delta_{tt'}(-1)^{t-1} \begin{Bmatrix} \frac{1}{2} & \frac{1}{2} & t \\ \frac{1}{2} & \frac{1}{2} & 1 \end{Bmatrix},$$

instead of $\boldsymbol{\tau}_2 \cdot \boldsymbol{\tau}_3$ as we do in Eq. (14). Either choice leads to an identical matrix element in the three-nucleon antisymmetrized basis (8). This is not the case once we regulate with the momentum transfer. Our choice in (12) results in the same isospin-coordinate structure as that obtained in [10].

2.4 Transformation of the momentum part of the NNN interaction

A general *NNN* interaction term is a product of isospin, spin and momentum parts. In this subsection, we manipulate the momentum part. We only consider the case of the regulator function $F(q^2, \Lambda)$ depending on the transferred momentum. The momentum part of a general term W_1 can be schematically written as

$$g_{K_1}(|\boldsymbol{Q}|; \Lambda) g_{K_2}(|\boldsymbol{Q}'|; \Lambda) (Y_{K_1}(\widehat{\boldsymbol{Q}}) Y_{K_2}(\widehat{\boldsymbol{Q}}'))^{(K)}, \tag{17}$$

with $K_1 + K_2$ even and with $\boldsymbol{Q}$ and $\boldsymbol{Q}'$ defined by Eqs. (3) and (4), respectively. For coordinates and momenta, $\widehat{\boldsymbol{Q}}$ denotes the angular part of the vector $\boldsymbol{Q}$. A transformation of (17) to coordinate space leads to a local interaction

$$\frac{1}{(2\pi)^6} \frac{1}{(\sqrt{3})^3} \int d\boldsymbol{\pi}_1\, d\boldsymbol{\pi}_2\, d\boldsymbol{\pi}_1'\, d\boldsymbol{\pi}_2'\, |\boldsymbol{\pi}_1 \boldsymbol{\pi}_2\rangle g_{K_1}(|\boldsymbol{Q}|; \Lambda) g_{K_2}(|\boldsymbol{Q}'|; \Lambda)$$
$$\times (Y_{K_1}(\widehat{\boldsymbol{Q}}) Y_{K_2}(\widehat{\boldsymbol{Q}}'))^{(K)} \langle \boldsymbol{\pi}_1' \boldsymbol{\pi}_2'|$$

$$= i^{K_1+K_2} \int d\boldsymbol{\xi}_1\, d\boldsymbol{\xi}_2\, |\boldsymbol{\xi}_1\boldsymbol{\xi}_2\rangle f_{K_1}(\sqrt{2}\xi_1;\Lambda) f_{K_2}\left(\left|\frac{1}{\sqrt{2}}\boldsymbol{\xi}_1 + \sqrt{\frac{3}{2}}\,\boldsymbol{\xi}_2\right|;\Lambda\right)$$
$$\times \left(Y_{K_1}(\hat{\xi}_1) Y_{K_2}\left(\widehat{\frac{1}{\sqrt{2}}\,\boldsymbol{\xi}_1 + \sqrt{\frac{3}{2}}\,\boldsymbol{\xi}_2}\right)\right)^{(K)} \langle \boldsymbol{\xi}_1\boldsymbol{\xi}_2|. \tag{18}$$

Using (1) and (2), we note that

$$\sqrt{2}\boldsymbol{\xi}_1 = \boldsymbol{r}_1 - \boldsymbol{r}_2 \qquad \text{and} \qquad \frac{1}{\sqrt{2}}\boldsymbol{\xi}_1 + \sqrt{\frac{3}{2}}\,\boldsymbol{\xi}_2 = \boldsymbol{r}_1 - \boldsymbol{r}_3.$$

In the above equation, we have introduced a new function using the relation

$$i^K f_K(r;\Lambda) Y_{Kk}(\hat{\boldsymbol{r}}) = \frac{1}{(2\pi)^3} \int d\boldsymbol{q} \exp[i\boldsymbol{q}\cdot\boldsymbol{r}]\, g_K(q;\Lambda) Y_{Kk}(\hat{\boldsymbol{q}}), \tag{19}$$

which implies

$$f_K(r;\Lambda) = \frac{1}{2\pi^2} \int dq\, q^2 j_K(qr) g_K(q;\Lambda). \tag{20}$$

We manipulate Eq. (18) first by utilizing the spherical harmonics relation

$$Y_{K_2k_2}(\widehat{\boldsymbol{r}_1 + \boldsymbol{r}_2}) = \sum_{K_3=0}^{K_2} \frac{\sqrt{4\pi}}{\widehat{K}_3} \left[\binom{2K_2+1}{2K_3}\right]^{1/2} r_1^{K_3} r_2^{K_2-K_3} |\boldsymbol{r}_1 + \boldsymbol{r}_2|^{-K_2}$$
$$\times \left(Y_{K_3}(\hat{\boldsymbol{r}}_1) Y_{K_2-K_3}(\hat{\boldsymbol{r}}_2)\right)^{(K_2)}_{k_2}, \tag{21}$$

and, second, by the following expansion involving the functions depending on $\left|(1/\sqrt{2})\boldsymbol{\xi}_1 + \sqrt{\frac{3}{2}}\boldsymbol{\xi}_2\right|$,

$$f_{K_2}(|\boldsymbol{r}_1 + \boldsymbol{r}_2|;\Lambda)|\boldsymbol{r}_1 + \boldsymbol{r}_2|^{-K_2} = 4\pi \sum_{XM_X} f_{K_2,X}(r_1, r_2;\Lambda)$$
$$\times (-1)^X Y^*_{XM_X}(\hat{\boldsymbol{r}}_1) Y_{XM_X}(\hat{\boldsymbol{r}}_2), \tag{22}$$

with the function $f_{K_2,X}(r_1, r_2;\Lambda)$ given by

$$f_{K_2,X}(r_1, r_2;\Lambda) = \frac{2}{\pi} \int dq\, q^2 j_X(qr_1) j_X(qr_2) \int dr\, r^2 j_0(qr) \frac{f_{K_2}(r;\Lambda)}{r^{K_2}}, \tag{23}$$

or, equivalently, by

$$f_{K_2,X}(r_1, r_2;\Lambda) = \frac{1}{2} \int_{-1}^{1} du\, P_X(u) \frac{f_{K_2}(\sqrt{r_1^2 + r_2^2 - 2r_1r_2u};\Lambda)}{(\sqrt{r_1^2 + r_2^2 - 2r_1r_2u})^{K_2}}. \tag{24}$$

Using (21) and (22), the term (18) is re-written in the form

$$= i^{K_1+K_2} \int d\boldsymbol{\xi}_1\, d\boldsymbol{\xi}_2\, |\boldsymbol{\xi}_1\boldsymbol{\xi}_2\rangle f_{K_1}(\sqrt{2}\xi_1;\Lambda) \sum_{K_3=0}^{K_2} \sum_{XYZV} \left[\binom{2K_2+1}{2K_3}\right]^{1/2}$$
$$\times \left(\frac{1}{\sqrt{2}}\,\xi_1\right)^{K_3} \left(\sqrt{\frac{3}{2}}\,\xi_2\right)^{K_2-K_3} f_{K_2,X}\left(\frac{1}{\sqrt{2}}\,\xi_1, \sqrt{\frac{3}{2}}\,\xi_2;\Lambda\right)$$

$$\times \widehat{X}^2 \widehat{K_2 - K_3} \widehat{K}_1 \widehat{K}_2 \widehat{Y} (-1)^{K_1+Y+Z+K} \left\{ \begin{array}{ccc} K_1 & Y & V \\ Z & K & K_2 \end{array} \right\}$$
$$\times \left\{ \begin{array}{ccc} Y & X & K_3 \\ K_2 - K_3 & K_2 & Z \end{array} \right\} (X0K_30|Y0)$$
$$\times (X0K_2 - K_30|Z0)(Y0K_10|V0)(Y_V(\hat{\xi}_1)Y_Z(\hat{\xi}_2))^{(K)}_k \langle \boldsymbol{\xi}_1 \boldsymbol{\xi}_2|, \tag{25}$$

which is convenient for matrix-element calculations.

2.5 One-pion exchange plus contact N^{2}LO NNN term

We are now in a position to discuss the one-pion exchange plus contact term that appears at the N^{2}LO. Following [11], we can write the W_1 term contribution as

$$W_1^{1\pi\text{-cont}} = -D \frac{1}{(2\pi)^6} \frac{g_A}{8F_\pi^2} \boldsymbol{\tau}_2 \cdot \boldsymbol{\tau}_3 \left[\frac{1}{\boldsymbol{Q}'^2 + M_\pi^2} \boldsymbol{\sigma}_2 \cdot \boldsymbol{Q}' \, \boldsymbol{\sigma}_3 \cdot \boldsymbol{Q}' \right.$$
$$\left. + \frac{1}{\boldsymbol{Q}^2 + M_\pi^2} \boldsymbol{\sigma}_2 \cdot \boldsymbol{Q} \, \boldsymbol{\sigma}_3 \cdot \boldsymbol{Q} \right], \tag{26}$$

with $D = c_D / F_\pi^2 \Lambda_\chi$, where c_D is an LEC from the chiral Lagrangian of order one. A diagrammatic depiction of the second term in the parenthesis is presented in Fig. 3. The first term corresponds to the exchange of $2 \leftrightarrow 3$.

Using the regulator dependent on the sum of Jacobi momenta squared of [11], this term can be cast in the form

$$W_1^{1\pi\text{-cont,ENGKMW}} = -D \frac{1}{(2\pi)^6} \frac{g_A}{8F_\pi^2} \frac{1}{(\sqrt{3})^3} \int d\boldsymbol{\pi}_1 \, d\boldsymbol{\pi}_2 \, d\boldsymbol{\pi}_1' \, d\boldsymbol{\pi}_2' |\boldsymbol{\pi}_1 \boldsymbol{\pi}_2\rangle$$
$$\times F\left(\frac{1}{2}(\pi_1^2 + \pi_2^2); \Lambda \right)$$
$$\times \boldsymbol{\tau}_2 \cdot \boldsymbol{\tau}_3 \left[\frac{1}{\boldsymbol{Q}'^2 + M_\pi^2} \boldsymbol{\sigma}_2 \cdot \boldsymbol{Q}' \boldsymbol{\sigma}_3 \cdot \boldsymbol{Q}' \right.$$
$$\left. + \frac{1}{\boldsymbol{Q}^2 + M_\pi^2} \boldsymbol{\sigma}_2 \cdot \boldsymbol{Q} \, \boldsymbol{\sigma}_3 \cdot \boldsymbol{Q} \right]$$
$$\times F\left(\frac{1}{2}(\pi_1'^2 + \pi_2'^2); \Lambda \right) \langle \boldsymbol{\pi}_1' \boldsymbol{\pi}_2' |. \tag{27}$$

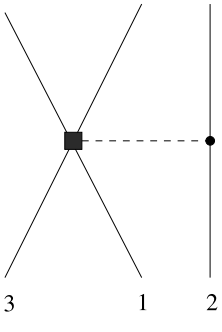

Fig. 3 One-pion exchange plus contact *NNN* interaction term of the N^{2}LO χEFT

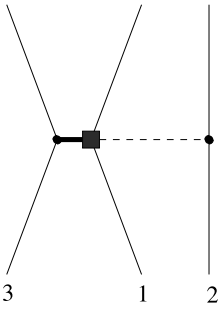

Fig. 4 One-pion exchange plus contact *NNN* interaction term of the N^{2}LO χEFT regulated by a function depending on momentum transfer

On the other hand, with a regulator dependent on momentum transfer, we get

$$W_1^{1\pi\text{-cont,Q}} = -D\frac{1}{(2\pi)^6}\frac{g_A}{8F_\pi^2}\frac{1}{(\sqrt{3})^3}\int d\boldsymbol{\pi}_1\, d\boldsymbol{\pi}_2\, d\boldsymbol{\pi}'_1\, d\boldsymbol{\pi}'_2\, |\boldsymbol{\pi}_1\boldsymbol{\pi}_2\rangle F(\boldsymbol{Q}^2;\Lambda) \times \boldsymbol{\tau}_2\cdot\boldsymbol{\tau}_3\left[\frac{1}{\boldsymbol{Q}'^2+M_\pi^2}\boldsymbol{\sigma}_2\cdot\boldsymbol{Q}'\boldsymbol{\sigma}_3\cdot\boldsymbol{Q}' + \frac{1}{\boldsymbol{Q}^2+M_\pi^2}\boldsymbol{\sigma}_2\cdot\boldsymbol{Q}\,\boldsymbol{\sigma}_3\cdot\boldsymbol{Q}\right] F(\boldsymbol{Q}'^2;\Lambda)\langle\boldsymbol{\pi}'_1\boldsymbol{\pi}'_2|, \tag{28}$$

which leads to a term local in coordinate space. We depict the second term in the parenthesis of (28) schematically in Fig. 4. The first term corresponds to the exchange of $2 \leftrightarrow 3$. This choice of regulation results in spin-isospin-coordinate structure that also appears in *NNN* terms obtained in [10]. We note that a somewhat different spin-isospin structure was used for one-pion exchange plus contact *NNN* terms in [32] and [34]. In [32] in particular, the $\boldsymbol{\sigma}$ and $\boldsymbol{\tau}$ operators were associated with the active nucleon 1, i.e.,

$$W_1^{1\pi\text{-cont,Q}_{\sigma_1}} = -D\frac{1}{(2\pi)^6}\frac{g_A}{8F_\pi^2}\frac{1}{(\sqrt{3})^3}\int d\boldsymbol{\pi}_1\, d\boldsymbol{\pi}_2\, d\boldsymbol{\pi}'_1\, d\boldsymbol{\pi}'_2\, |\boldsymbol{\pi}_1\boldsymbol{\pi}_2\rangle F(\boldsymbol{Q}^2;\Lambda) \times \left[\boldsymbol{\tau}_1\cdot\boldsymbol{\tau}_3\frac{1}{\boldsymbol{Q}'^2+M_\pi^2}\boldsymbol{\sigma}_1\cdot\boldsymbol{Q}'\,\boldsymbol{\sigma}_3\cdot\boldsymbol{Q}' + \boldsymbol{\tau}_1\cdot\boldsymbol{\tau}_2\frac{1}{\boldsymbol{Q}^2+M_\pi^2}\boldsymbol{\sigma}_1\cdot\boldsymbol{Q}\,\boldsymbol{\sigma}_2\cdot\boldsymbol{Q}\right] F(\boldsymbol{Q}'^2;\Lambda)\langle\boldsymbol{\pi}'_1\boldsymbol{\pi}'_2|. \tag{29}$$

This change does not alter the matrix element of (27) in the antisymmetrized three-nucleon basis. It will lead to a difference in the matrix element of (28). However, the dependence on the regulator is a higher-order effect than the χEFT expansion order used to derive the *NNN* interaction. Therefore, these differences should have only a minor overall effect. In fact, we confirmed in nuclear structure calculations such as those described in [14] that the impact of the choice (27) or (28) is small in particular when the natural LECs values are used ($|c_D| \approx 1$). However, a more significant impact of the choice of the regulator in particular on spin-orbit force sensitive observables is observed in the case of the two-pion-exchange terms as discussed in the Introduction.

Due to the antisymmetry of the three-nucleon wave functions in (8), it is sufficient to consider just one term of the two in parenthesis in (27) and (28) and multiply the result by 2. Using the first term, the matrix element of (27) with the regulator dependent on the sum of Jacobi momenta squared is obtained in the form

$$
\begin{aligned}
&\langle (nlsjt,\mathcal{N}\mathcal{L}\mathcal{J})JT|W_1^{1\pi\text{-cont,ENGKMW}}|(n'l's'j't',\mathcal{N}'\mathcal{L}'\mathcal{J}')JT\rangle \\
&\quad = -D\frac{g_A}{F_\pi^2}\frac{1}{2\sqrt{3}\pi^4}\delta_{l0}\delta_{l'0}\delta_{sj}\delta_{s'j'}\hat{t}\hat{t}'\begin{Bmatrix} t & t' & 1 \\ \frac{1}{2} & \frac{1}{2} & \frac{1}{2}\end{Bmatrix}\begin{Bmatrix} t & t' & 1 \\ \frac{1}{2} & \frac{1}{2} & T\end{Bmatrix} \\
&\qquad \times (-1)^{(n+\mathcal{N}+n'+\mathcal{N}')+(\mathcal{L}+\mathcal{L}')/2} \\
&\qquad \times \hat{j}\hat{j}'\hat{\mathcal{J}}\hat{\mathcal{J}}'(-1)^{J-\mathcal{J}+T+\frac{1}{2}}\begin{Bmatrix} j & j' & 1 \\ \frac{1}{2} & \frac{1}{2} & \frac{1}{2}\end{Bmatrix}\begin{Bmatrix} j & j' & 1 \\ \mathcal{J}' & \mathcal{J} & J\end{Bmatrix} \\
&\qquad \times \sum_{K=0,2}\hat{K}(1010|K0)\begin{Bmatrix} \mathcal{J} & \mathcal{L} & \frac{1}{2} \\ \mathcal{J}' & \mathcal{L}' & \frac{1}{2} \\ 1 & K & 1\end{Bmatrix} \\
&\qquad \times \sum_{K_1=0}^{K}\widehat{K-K_1}\left[\begin{pmatrix} 2K+1 \\ 2K_1\end{pmatrix}\right]^{1/2}(-1)^{\mathcal{L}+K_1}\sum_X \hat{X}\hat{\mathcal{L}}'(K_10X0|\mathcal{L}0) \\
&\qquad \times (\mathcal{L}'0K-K_10|X0)\begin{Bmatrix} \mathcal{L}' & K-K_1 & X \\ K_1 & \mathcal{L} & K\end{Bmatrix} \\
&\qquad \times \int d\pi_1\, d\pi_2\, d\pi_1'\, d\pi_2' \pi_1^2\pi_2^2\pi_1'^2\pi_2'^2 R_{n0}(\pi_1,1/b)R_{\mathcal{N}\mathcal{L}}(\pi_2,1/b)F\left(\frac{1}{2}(\pi_1^2+\pi_2^2);\Lambda\right) \\
&\qquad \times R_{n'0}(\pi_1',1/b)R_{\mathcal{N}'\mathcal{L}'}(\pi_2',1/b)F\left(\frac{1}{2}(\pi_1'^2+\pi_2'^2);\Lambda\right)\pi_2^{K_1}\pi_2'^{K-K_1}g_{K,X}(\pi_2,\pi_2'),
\end{aligned}
\tag{30}
$$

where we introduced the function

$$
g_{K,X}(p,p') = \frac{2}{\pi}\int dq\, q^2\, dr\, r^2\, \frac{q^{2-K}}{\frac{2}{3}q^2+M_\pi^2}j_0(qr)j_X(pr)j_X(p'r), \tag{31}
$$

which can be alternatively evaluated through

$$
g_{K,X}(p,p') = \frac{1}{2}\int_{-1}^{1} du\, P_X(u)\,\frac{\sqrt{p^2+p'^2-2pp'u}^{2-K}}{\frac{2}{3}(p^2+p'^2-2pp'u)^2+M_\pi^2}. \tag{32}
$$

The matrix element (30) was first derived in [11].

For the one-pion exchange plus contact term (28) with the regulator dependent on momentum transfer, we present the matrix element obtained using both terms in the parenthesis of (28). Due to the three-nucleon wave-function antisymmetry, both contributions lead to the same result for (8). One can take the advantage of this

feature and use the alternative calculations to check the correctness of the numerical code. First, we take the first part of (28) and get

$$
\begin{aligned}
&\langle (nlsjt, \mathcal{NLJ})JT | W_1^{1\pi\text{-cont,Q}} | (n'l's'j't', \mathcal{N}'\mathcal{L}'\mathcal{J}')JT \rangle \\
&\quad = -D\frac{9g_A}{F_\pi^2}\hat{t}\hat{t}'(-1)^{t+t'+T+\frac{1}{2}}
\begin{Bmatrix} t & t' & 1 \\ \frac{1}{2} & \frac{1}{2} & \frac{1}{2} \end{Bmatrix}
\begin{Bmatrix} t & t' & 1 \\ \frac{1}{2} & \frac{1}{2} & T \end{Bmatrix} \\
&\qquad \times \hat{j}\hat{j}'\hat{\mathcal{J}}\hat{\mathcal{J}}'(-1)^{J-\mathcal{J}+s+j'}
\begin{Bmatrix} s & s' & 1 \\ \frac{1}{2} & \frac{1}{2} & \frac{1}{2} \end{Bmatrix} \\
&\qquad \times \sum_{K=0,2} \hat{K}(-1)^{(K/2)}(1010|K0) \sum_{K_2,K_3} \hat{K}_2\hat{K}_3\hat{l}'\hat{\mathcal{L}}'(l'0K_20|l0)(\mathcal{L}'0K_30|\mathcal{L}0) \\
&\qquad \times \sum_Z \hat{Z}^2
\begin{Bmatrix} l & s & j \\ l' & s' & j' \\ K_2 & 1 & Z \end{Bmatrix}
\begin{Bmatrix} \mathcal{L} & \frac{1}{2} & \mathcal{J} \\ \mathcal{L}' & \frac{1}{2} & \mathcal{J}' \\ K_3 & 1 & Z \end{Bmatrix} \\
&\qquad \times \begin{Bmatrix} j & j' & Z \\ \mathcal{J}' & \mathcal{J} & J \end{Bmatrix}
\begin{Bmatrix} K_2 & 1 & Z \\ 1 & K_3 & K \end{Bmatrix} \\
&\qquad \times \sum_{K_1=0}^{K} \widehat{K-K_1}\left[\binom{2K+1}{2K_1}\right]^{1/2}(-1)^{K_1}\sum_X (-1)^X \hat{X}^2 (K_10X0|K_20) \\
&\qquad \times (K-K_10X0|K_30)
\begin{Bmatrix} K_1 & X & K_2 \\ K_3 & K & K-K_1 \end{Bmatrix} \\
&\qquad \times \int d\xi_1\, d\xi_2\, \xi_1^2\xi_2^2 R_{nl}(\xi_1,b) R_{\mathcal{NL}}(\xi_2,b) R_{n'l'}(\xi_1,b) R_{\mathcal{N}'\mathcal{L}'}(\xi_2,b) \\
&\qquad \times \left(\sqrt{\frac{1}{2}}\xi_1\right)^{K_1}\left(\sqrt{\frac{3}{2}}\xi_2\right)^{K-K_1} Z_0(\sqrt{2}\xi_1;\Lambda) f_{K,X}\left(\sqrt{\frac{1}{2}}\xi_1, \sqrt{\frac{3}{2}}\xi_2;\Lambda\right),
\end{aligned}
\tag{33}
$$

with the functions

$$
f_{0,X}(r_1,r_2;\Lambda) = \frac{1}{2\pi^2}\int dq\, q^2 j_X(qr_1) j_X(qr_2) \frac{q^2 F(q^2;\Lambda)}{q^2+M_\pi^2} \tag{34}
$$

and

$$
f_{2,X}(r_1,r_2;\Lambda) = \frac{1}{4\pi^2}\int_0^\infty dq\, q^2 j_X(qr_1) j_X(qr_2) \int_q^\infty dk\, k(k^2-q^2)\frac{F(k^2;\Lambda)}{k^2+M_\pi^2}, \tag{35}
$$

which are special cases of (23). An alternative way of evaluating (35) is

$$
f_{2,X}(r_1,r_2;\Lambda) = \frac{1}{2}\int_{-1}^{1} du\, P_X(u) \frac{f_2(\sqrt{r_1^2+r_2^2-2r_1r_2u};\Lambda)}{r_1^2+r_2^2-2r_1r_2u}, \tag{36}
$$

with

$$
f_2(r;\Lambda) = \frac{1}{2\pi^2}\int dq\, q^2 j_2(qr)\frac{q^2F(q^2;\Lambda)}{q^2+M_\pi^2}. \tag{37}
$$

We note that (36) is numerically more efficient than (35).

Next, we take the second part of (28), which results in a simpler expression for one-pion exchange plus contact N^{2}LO three-nucleon matrix element in non-anti-symmetrized basis,

$$
\begin{aligned}
&\langle (nlsjt, \mathcal{N}\mathcal{L}\mathcal{J})JT | W_1^{1\pi\text{-cont,Q}} | (n'l's'j't', \mathcal{N}'\mathcal{L}'\mathcal{J}')JT \rangle \\
&\quad = -D\frac{9g_A}{F_\pi^2}\hat{t}\hat{t}'(-1)^{t+t'+T+\frac{1}{2}}
\begin{Bmatrix} t & t' & 1 \\ \frac{1}{2} & \frac{1}{2} & \frac{1}{2} \end{Bmatrix}
\begin{Bmatrix} t & t' & 1 \\ \frac{1}{2} & \frac{1}{2} & T \end{Bmatrix} \\
&\qquad \times \hat{j}\hat{j}'\hat{\mathcal{J}}\hat{\mathcal{J}}'\hat{s}\hat{s}'(-1)^{J-\mathcal{J}+s+j'}
\begin{Bmatrix} s & s' & 1 \\ \frac{1}{2} & \frac{1}{2} & \frac{1}{2} \end{Bmatrix}
\hat{l}'\hat{\mathcal{L}}' \\
&\qquad \times \sum_{K=0,2} \hat{K}(-1)^{(K/2)}(1010|K0) \sum_V (-1)^V \hat{V}(V0l'0|l0) \\
&\qquad \times \sum_X \hat{X}^2 (X0K0|V0)(X0\mathcal{L}'0|\mathcal{L}0) \\
&\qquad \times \sum_Z \hat{Z}^2
\begin{Bmatrix} l & s & j \\ l' & s' & j' \\ V & 1 & Z \end{Bmatrix}
\begin{Bmatrix} \mathcal{L} & \frac{1}{2} & \mathcal{J} \\ \mathcal{L}' & \frac{1}{2} & \mathcal{J}' \\ X & 1 & Z \end{Bmatrix}
\begin{Bmatrix} j & j' & Z \\ \mathcal{J}' & \mathcal{J} & J \end{Bmatrix}
\begin{Bmatrix} V & 1 & Z \\ 1 & X & K \end{Bmatrix} \\
&\qquad \times \int d\xi_1\, d\xi_2\, \xi_1^2 \xi_2^2 R_{nl}(\xi_1, b) R_{\mathcal{N}\mathcal{L}}(\xi_2, b) R_{n'l'}(\xi_1, b) R_{\mathcal{N}'\mathcal{L}'}(\xi_2, b) \\
&\qquad \times f_K(\sqrt{2}\xi_1; \Lambda) Z_{0,X}\left(\sqrt{\frac{1}{2}}\xi_1, \sqrt{\frac{3}{2}}\xi_2; \Lambda\right),
\end{aligned}
\tag{38}
$$

with

$$
f_K(r;\Lambda) = \frac{1}{2\pi^2}\int dq\, q^2 j_K(qr)\frac{q^2 F(q^2;\Lambda)}{q^2 + M_\pi^2}, \tag{39}
$$

which is a special case of (20) and $Z_{0,X}(r_1, r_2; \Lambda)$ given by Eq. (16). Both (33) and (38) are already multiplied by 2 in anticipation of the three-nucleon antisymmetry in the final matrix element (8).

For completeness, we also present the matrix element of the second part of (29),

$$
\begin{aligned}
&\langle (nlsjt, \mathcal{N}\mathcal{L}\mathcal{J})JT | W_1^{1\pi\text{-cont,Q}_{\sigma_1}} | (n'l's'j't', \mathcal{N}'\mathcal{L}'J')JT \rangle \\
&\quad = -D\frac{9g_A}{F_\pi^2}\delta_{tt'}(-1)^{t-1}
\begin{Bmatrix} \frac{1}{2} & \frac{1}{2} & t \\ \frac{1}{2} & \frac{1}{2} & 1 \end{Bmatrix}
\hat{j}\hat{j}'\hat{\mathcal{J}}\hat{\mathcal{J}}'\hat{s}\hat{s}'\hat{l}'\hat{\mathcal{L}}'(-1)^{s+s'+j'+J+\mathcal{L}+\mathcal{J}+\mathcal{J}'+\frac{1}{2}} \\
&\qquad \times \sum_{K=0,2} \hat{K}(-1)^{(K/2)}(1010|K0)
\begin{Bmatrix} s & s' & K \\ \frac{1}{2} & \frac{1}{2} & 1 \\ \frac{1}{2} & \frac{1}{2} & 1 \end{Bmatrix}
\sum_V \hat{V}(V0l'0|l0) \\
&\qquad \times \sum_X \hat{X}^2 (X0K0|V0)(X0\mathcal{L}'0|\mathcal{L}0) \\
&\qquad \times
\begin{Bmatrix} l & s & j \\ l' & s' & j' \\ V & K & X \end{Bmatrix}
\begin{Bmatrix} \mathcal{J} & X & \mathcal{J}' \\ j' & J & j \end{Bmatrix}
\begin{Bmatrix} \mathcal{J} & X & \mathcal{J}' \\ \mathcal{L}' & \frac{1}{2} & \mathcal{L} \end{Bmatrix}
\end{aligned}
$$

$$\times \int d\xi_1\, d\xi_2\, \xi_1^2 \xi_2^2 R_{nl}(\xi_1, b) R_{\mathcal{NL}}(\xi_2, b) R_{n'l'}(\xi_1, b) R_{\mathcal{N}'\mathcal{L}'}(\xi_2, b)$$
$$\times f_K(\sqrt{2}\xi_1; \Lambda) Z_{0,X}\left(\sqrt{\frac{1}{2}}\xi_1, \sqrt{\frac{3}{2}}\xi_2; \Lambda\right), \tag{40}$$

which is still simpler than (38). Again, this matrix element is already multiplied by 2 in anticipation of the three-nucleon antisymmetry in the final matrix element (8). The matrix element of (two-times the) first part of (29) is given by (33) multiplied by $(-1)^{t+t'+s+s'}$. Due to the three-nucleon wave-function antisymmetry, this contribution leads to the same result for (8) as does (38), which can be taken advantage of in testing the correctness of numerical calculations.

By comparing (27) with (33) (or equivalently with (38) and also with (40)) we note the different tensorial structure of the matrix elements. When the regulator dependent on the sum of Jacobi momenta squared is used, only the $l = 0$, $l' = 0$ partial waves contribute. This is not the case, when the regulator depending on momentum transfer is utilized. At the same time, however, we note that in the limit $\Lambda \to \infty$ both expressions (27) and (33) as well as (38) and (40) lead to the same result.

2.6 Two-pion exchange N^{2}LO NNN terms

In this subsection, we present matrix elements of two-pion exchange N^{2}LO *NNN* terms. Their schematic depiction is shown in Fig. 5. There are three distinct terms associated with three LECs, c_1, c_3 and c_4, from the chiral Lagrangian, which also appear in the sub-leading two-pion exchange in the *NN* potential. Consequently, values of these LECs expected to be of order one are typically fixed at the *NN* level unlike the case of the previously introduced c_D (26) and c_E (9) LECs whose values need to be fixed in systems of more than two nucleons. In the present paper, we derive only the matrix elements of the two-pion exchange *NNN* interaction terms regulated by a function depending on momentum transfer, i.e., terms that are local in coordinate space.

Following [11], the W_1 part of the c_1 term with the momentum transfer regulators can be written as

$$W_1^{2\pi\text{-c1}} = -c_1 \frac{1}{(2\pi)^6} \frac{4M_\pi^2}{F_\pi^2} \frac{g_A^2}{4F_\pi^2} \boldsymbol{\tau}_2 \cdot \boldsymbol{\tau}_3 F(\boldsymbol{Q}^2; \Lambda) \frac{1}{\boldsymbol{Q}^2 + M_\pi^2} \boldsymbol{\sigma}_2 \cdot \boldsymbol{Q}$$
$$\times \boldsymbol{\sigma}_3 \cdot \boldsymbol{Q}' \frac{1}{\boldsymbol{Q}'^2 + M_\pi^2} F(\boldsymbol{Q}'^2; \Lambda). \tag{41}$$

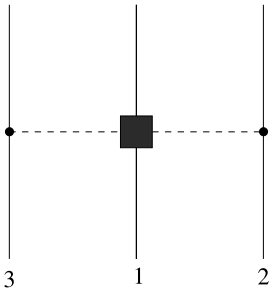

Fig. 5 Two-pion exchange *NNN* interaction term of the N^{2}LO χEFT

Using results of Subsect. 2.4, we find for the c_1-term matrix element

$$\begin{aligned}
&\langle (nlsjt,\mathcal{NLJ})JT|W_1^{2\pi\text{-c1,Q}}|(n'l's'j't',\mathcal{N}'\mathcal{L}'\mathcal{J}')JT\rangle \\
&\quad = -c_1\frac{36M_\pi^2}{F_\pi^2}\frac{g_A^2}{F_\pi^2}\hat{t}\hat{t}'(-1)^{t+t'+T+\frac{1}{2}}\begin{Bmatrix} t & t' & 1\\ \frac{1}{2} & \frac{1}{2} & \frac{1}{2}\end{Bmatrix}\begin{Bmatrix} t & t' & 1\\ \frac{1}{2} & \frac{1}{2} & T\end{Bmatrix} \\
&\qquad \times \hat{j}\hat{j}'\hat{\mathcal{J}}\hat{\mathcal{J}}'\hat{s}\hat{s}'(-1)^{J-\mathcal{J}+s+j'}\begin{Bmatrix} s & s' & 1\\ \frac{1}{2} & \frac{1}{2} & \frac{1}{2}\end{Bmatrix}\hat{l}'\hat{\mathcal{L}}' \\
&\qquad \times \sum_{VR}\hat{V}\hat{R}(V0l'0|l0)(R0\mathcal{L}'0|\mathcal{L}0)\sum_Y(-1)^Y\hat{Y}(Y010|V0)\begin{Bmatrix} l & s & j\\ l' & s' & j'\\ V & 1 & Y\end{Bmatrix} \\
&\qquad \times \begin{Bmatrix} \mathcal{L} & \frac{1}{2} & \mathcal{J}\\ \mathcal{L}' & \frac{1}{2} & \mathcal{J}'\\ R & 1 & Y\end{Bmatrix}\begin{Bmatrix} j & j' & Y\\ \mathcal{J}' & \mathcal{J} & J\end{Bmatrix} \\
&\qquad \times \sum_{K_3=0}^{1}\left[\binom{3}{2K_3}\right]^{1/2}\widehat{1-K_3}\sum_X\hat{X}^2(X0K_30|Y0)(X01-K_30|R0) \\
&\qquad \times \begin{Bmatrix} Y & X & K_3\\ 1-K_3 & 1 & R\end{Bmatrix} \\
&\qquad \times \int d\xi_1\,d\xi_2\,\xi_1^2\xi_2^2R_{nl}(\xi_1,b)R_{\mathcal{NL}}(\xi_2,b)R_{n'l'}(\xi_1,b)R_{\mathcal{N}'\mathcal{L}'}(\xi_2,b) \\
&\qquad \times \left(\sqrt{\frac{1}{2}}\xi_1\right)^{K_3}\left(\sqrt{\frac{3}{2}}\xi_2\right)^{1-K_3}f_1(\sqrt{2}\xi_1;\Lambda)f_{1,X}\left(\sqrt{\frac{1}{2}}\xi_1,\sqrt{\frac{3}{2}}\xi_2;\Lambda\right). \qquad (42)
\end{aligned}$$

Here we introduced the functions

$$f_1(r;\Lambda)=\frac{1}{2\pi^2}\int dq\,q^2j_1(q)\frac{qF(q^2;\Lambda)}{q^2+M_\pi^2} \qquad (43)$$

and

$$f_{1,X}(r_1,r_2;\Lambda)=\frac{1}{2\pi^2}\int_0^\infty dq\,q^2j_X(qr_1)j_X(qr_2)\int_q^\infty dk\frac{kF(k^2;\Lambda)}{k^2+M_\pi^2}, \qquad (44)$$

which are the explicit versions of functions given in Eqs. (20) and (23), respectively. The function (44) can be alternatively evaluated with the help of the Legendre polynomial,

$$f_{1,X}(r_1,r_2;\Lambda)=\frac{1}{2}\int_{-1}^1 du\,P_X(u)\frac{f_1(\sqrt{r_1^2+r_2^2-2r_1r_2u};\Lambda)}{\sqrt{r_1^2+r_2^2-2r_1r_2u}}. \qquad (45)$$

The W_1 part of the two-pion exchange c_3 term is given by [11]

$$\begin{aligned}
W_1^{2\pi\text{-c3}} &= c_3\frac{1}{(2\pi)^6}\frac{2}{F_\pi^2}\frac{g_A^2}{4F_\pi^2}\boldsymbol{\tau}_2\cdot\boldsymbol{\tau}_3\,F(\boldsymbol{Q}^2;\Lambda)\frac{1}{\boldsymbol{Q}^2+M_\pi^2}\boldsymbol{\sigma}_2\cdot\boldsymbol{Q}\,\boldsymbol{\sigma}_3\cdot\boldsymbol{Q}' \\
&\quad \times\boldsymbol{Q}\cdot\boldsymbol{Q}'\frac{1}{\boldsymbol{Q}'^2+M_\pi^2}F(\boldsymbol{Q}'^2;\Lambda). \qquad (46)
\end{aligned}$$

For its matrix element we find

$$
\begin{aligned}
&\langle (nlsjt,\mathcal{NLJ})JT|W_1^{2\pi\_c3,\mathrm{Q}}|(n'l's'j't',\mathcal{N}'\mathcal{L}'\mathcal{J}')JT\rangle \\
&\quad = c_3\frac{18}{F_\pi^2}\frac{g_A^2}{F_\pi^2}\hat{t}\hat{t}'(-1)^{t+t'+T+\frac{1}{2}}\left\{\begin{array}{ccc} t & t' & 1 \\ \frac{1}{2} & \frac{1}{2} & \frac{1}{2}\end{array}\right\}\left\{\begin{array}{ccc} t & t' & 1 \\ \frac{1}{2} & \frac{1}{2} & T\end{array}\right\} \\
&\qquad \times \hat{j}\hat{j}'\hat{\mathcal{J}}\hat{\mathcal{J}}'\hat{s}\hat{s}'(-1)^{J-\mathcal{J}+s+j'}\left\{\begin{array}{ccc} s & s' & 1 \\ \frac{1}{2} & \frac{1}{2} & \frac{1}{2}\end{array}\right\}\hat{l}'\hat{\mathcal{L}}' \\
&\qquad \times \sum_{K_1K_2}(-1)^{(K_1+K_2)/2}\widehat{K}_1\widehat{K}_2(1010|K_10)(1010|K_20) \\
&\qquad \times \sum_{VR}(-1)^{V+R}\widehat{V}\widehat{R}(V0l'0|l0)(R0\mathcal{L}'0|\mathcal{L}0)\sum_Y \widehat{Y}(Y0K_10|V0) \\
&\qquad \times \sum_Z \widehat{Z}^2(-1)^Z\left\{\begin{array}{ccc} l & s & j \\ l' & s' & j' \\ V & 1 & Z\end{array}\right\}\left\{\begin{array}{ccc} \mathcal{L} & \frac{1}{2} & \mathcal{J} \\ \mathcal{L}' & \frac{1}{2} & \mathcal{J}' \\ R & 1 & Z\end{array}\right\}\left\{\begin{array}{ccc} j & j' & Z \\ \mathcal{J}' & \mathcal{J} & J\end{array}\right\} \\
&\qquad \times \left\{\begin{array}{ccc} Z & 1 & Y \\ K_1 & V & 1\end{array}\right\}\left\{\begin{array}{ccc} Z & 1 & Y \\ K_2 & R & 1\end{array}\right\} \\
&\qquad \times \sum_{K_3=0}^{K_2}\left[\binom{2K_2+1}{2K_3}\right]^{1/2}\widehat{K_2-K_3}\sum_X \widehat{X}^2(X0K_30|Y0) \\
&\qquad \times (X0K_2-K_30|R0)\left\{\begin{array}{ccc} Y & X & K_3 \\ K_2-K_3 & K_2 & R\end{array}\right\} \\
&\qquad \times \int d\xi_1\,d\xi_2\,\xi_1^2\xi_2^2 R_{nl}(\xi_1,b)R_{\mathcal{NL}}(\xi_2,b)R_{n'l'}(\xi_1,b)R_{\mathcal{N}'\mathcal{L}'}(\xi_2,b) \\
&\qquad \times \left(\sqrt{\frac{1}{2}}\xi_1\right)^{K_3}\left(\sqrt{\frac{3}{2}}\xi_2\right)^{K_2-K_3} f_{K_1}(\sqrt{2}\xi_1;\Lambda)f_{K_2,X}\left(\sqrt{\frac{1}{2}}\xi_1,\sqrt{\frac{3}{2}}\xi_2;\Lambda\right), \qquad (47)
\end{aligned}
$$

with the function $f_{K_1}(r;\Lambda)$ given by (39), the function $f_{0,X}(r_1,r_2;\Lambda)$ given by (34) and the function $f_{2,X}(r_1,r_2;\Lambda)$ given by (35).

Finally, the W_1 part of the two-pion exchange c_4 term is given by [11]

$$
\begin{aligned}
W_1^{2\pi\_c4} &= c_4\frac{1}{(2\pi)^6}\frac{1}{F_\pi^2}\frac{g_A^2}{4F_\pi^2}\boldsymbol{\tau}_1\cdot(\boldsymbol{\tau}_2\times\boldsymbol{\tau}_3)F(\boldsymbol{Q}^2;\Lambda)\frac{1}{\boldsymbol{Q}^2+M_\pi^2}\boldsymbol{\sigma}_2\cdot\boldsymbol{Q}\,\boldsymbol{\sigma}_3\cdot\boldsymbol{Q}' \\
&\quad \times \boldsymbol{\sigma}_1\cdot(\boldsymbol{Q}\times\boldsymbol{Q}')\frac{1}{\boldsymbol{Q}'^2+M_\pi^2}F(\boldsymbol{Q}'^2;\Lambda), \qquad (48)
\end{aligned}
$$

and for its matrix element we find

$$
\begin{aligned}
&\langle (nlsjt,\mathcal{NLJ})JT|W_1^{2\pi\_c4,\mathrm{Q}}|(n'l's'j't',\mathcal{N}'\mathcal{L}'\mathcal{J}')JT\rangle \\
&\qquad = -c_4\frac{36^2}{F_\pi^2}\frac{g_A^2}{4F_\pi^2}\hat{t}\hat{t}'(-1)^{T+t'+\frac{1}{2}}\left\{\begin{array}{ccc} t & t' & 1 \\ \frac{1}{2} & \frac{1}{2} & T\end{array}\right\}\left\{\begin{array}{ccc} \frac{1}{2} & \frac{1}{2} & t' \\ \frac{1}{2} & \frac{1}{2} & t \\ 1 & 1 & 1\end{array}\right\}
\end{aligned}
$$

$$
\begin{aligned}
&\times \widehat{j}\widehat{j}'\widehat{\mathcal{J}}\widehat{\mathcal{J}}'\hat{s}\hat{s}'(-1)^{J+\mathcal{J}+j'}\hat{l}'\widehat{\mathcal{L}}' \\
&\times \sum_{K_1K_2}(-1)^{(K_1+K_2)/2}\widehat{K}_1\widehat{K}_2(1010|K_10)(1010|K_20) \\
&\times \sum_{VR}(-1)^{V+R}\widehat{V}\widehat{R}(V0l'0|l0)(R0\mathcal{L}'0|\mathcal{L}0)\sum_{Y}\widehat{Y}(Y0K_10|V0) \\
&\times \sum_{Z}\widehat{Z}^2(-1)^{Z}\begin{Bmatrix} \mathcal{L} & \frac{1}{2} & \mathcal{J} \\ \mathcal{L}' & \frac{1}{2} & \mathcal{J}' \\ R & 1 & Z \end{Bmatrix}\begin{Bmatrix} j & j' & Z \\ \mathcal{J}' & \mathcal{J} & J \end{Bmatrix}\begin{Bmatrix} Z & 1 & Y \\ K_2 & R & 1 \end{Bmatrix} \\
&\times \sum_{K_4}\widehat{K}_4^2\begin{Bmatrix} l & s & j \\ l' & s' & j' \\ V & K_4 & Z \end{Bmatrix}\begin{Bmatrix} \frac{1}{2} & \frac{1}{2} & s \\ \frac{1}{2} & \frac{1}{2} & s' \\ 1 & 1 & K_4 \end{Bmatrix}\begin{Bmatrix} Z & 1 & Y \\ K_1 & V & K_4 \end{Bmatrix} \\
&\times \begin{Bmatrix} 1 & 1 & 1 \\ 1 & K_4 & K_1 \end{Bmatrix} \\
&\times \sum_{K_3=0}^{K_2}\left[\binom{2K_2+1}{2K_3}\right]^{1/2}\widehat{K_2-K_3}\sum_{X}\widehat{X}^2(X0K_30|Y0) \\
&\times (X0K_2-K_30|R0)\begin{Bmatrix} Y & X & K_3 \\ K_2-K_3 & K_2 & R \end{Bmatrix} \\
&\times \int d\xi_1\, d\xi_2\, \xi_1^2\xi_2^2 R_{nl}(\xi_1,b)R_{\mathcal{N}\mathcal{L}}(\xi_2,b)R_{n'l'}(\xi_1,b)R_{\mathcal{N}'\mathcal{L}'}(\xi_2,b) \\
&\times \left(\sqrt{\frac{1}{2}}\xi_1\right)^{K_3}\left(\sqrt{\frac{3}{2}}\xi_2\right)^{K_2-K_3} f_{K_1}\left(\sqrt{2}\xi_1;\Lambda\right) f_{K_2,X}\left(\sqrt{\frac{1}{2}}\xi_1,\sqrt{\frac{3}{2}}\xi_2;\Lambda\right). \quad (49)
\end{aligned}
$$

The same functions (34), (35) and (39) that were introduced in the c_3 term enter the c_4 term as well.

We note that the local two-pion-exchange terms appear also in the Tucson-Melbourne *NNN* interaction [20]. The analogous terms to c_1, c_3 and c_4 are present in particular in the TM′ interaction [21, 22]. The TM′ parameters are denoted by a', b and d with the relation to the above c_1, c_3 and c_4 given by

$$a' = \frac{4M_\pi^2}{F_\pi^2}c_1, \quad (50)$$

$$b = \frac{2}{F_\pi^2}c_3, \quad (51)$$

$$d = \frac{-1}{F_\pi^2}c_4. \quad (52)$$

Further, the regulator function $F(q^2;\Lambda)$ is chosen in the form

$$F^{\mathrm{TM}}(q^2;\Lambda) = \frac{\Lambda^2 - M_\pi^2}{\Lambda^2 + q^2}. \quad (53)$$

This choice allows to evaluate integrals that define the functions f_K analytically. The analytic expressions can be found, e.g., in [29]. In that paper, the following function is introduced,

$$Z_1(r;\Lambda) = \frac{1}{2\pi^2}\int dq\, q^2 j_0(qr)\frac{F(q^2;\Lambda)}{q^2+M_\pi^2}. \tag{54}$$

Using the properties of spherical Bessel functions, we can easily find relations between derivatives of Z_1 and our f_K functions,

$$f_0(r,\Lambda) = -\left(Z_1''(r;\Lambda) + \frac{2}{r}Z_1'(r;\Lambda)\right), \tag{55}$$

$$f_1(r,\Lambda) = -Z_1'(r;\Lambda), \tag{56}$$

$$f_2(r,\Lambda) = Z_1''(r;\Lambda) - \frac{1}{r}Z_1'(r;\Lambda). \tag{57}$$

For completeness, we note that a still different notation was used in [10], where functions $I_{k,l}(r;\Lambda)$ were introduced. They are related to the $Z_0(r,\Lambda)$ that we introduced in Eq. (13) and to the above Z_1 function (54) it is as follows,

$$Z_0(r,\Lambda) = I_{0,0}(r;\Lambda), \tag{58}$$

$$Z_1(r,\Lambda) = I_{2,0}(r,\Lambda). \tag{59}$$

In [37], the Tucson-Melbourne *NNN* interaction matrix elements in the HO basis were calculated using a different algorithm than the one used in this paper. That algorithm relied on a completeness relation and on transformations of HO states with the help of HO brackets. Even though the algorithm of [37] required a calculation of one-dimensional radial integrals, while the present algorithm requires evaluation of two-dimensional radial integrals, the present algorithm is substantially more efficient.

3 Convergence test for ^{3}H and ^{4}He

In this section, we apply the matrix elements of the N^{2}LO χEFT *NNN* interaction obtained in this paper to the NCSM calculation of ^{3}H and ^{4}He ground-state properties. As a test of correctness of the computer code, we verified that the new more efficient algorithm reproduces the results obtained using the algorithm of [37] for the two-pion-exchange term matrix elements. For the contact terms, we verified that in the limit of $\Lambda \to \infty$, the matrix elements (15) and (14) lead to the same result and the same is true for matrix elements (38) and (30). In addition, we benchmarked the computer code for evaluation of (14) and (30) with the computer code written by A. Nogga [38]. Finally, we tested numerically that the use of (33) results in the same matrix element as the use of (38) in the three-nucleon antisymmetrized basis $|NiJT\rangle$ introduced in Eq. (8). The same checks were also performed for the alternative version of the one-pion-exchange plus contact term (*D*-term) given in Eq. (29). That is, we verified numerically that the matrix element (40) leads to the same result as (30) in the limit of $\Lambda \to \infty$ and the use of (40) results in the same matrix element in the three-nucleon antisymmetrized basis $|NiJT\rangle$ as the use of (33) multiplied by $(-1)^{t+t'+s+s'}$.

We use the N^{3}LO *NN* interaction of [13]. We adopt the c_1, c_3 and c_4 LEC values as well as the value of Λ from the N^{3}LO *NN* interaction of [13] for our local chiral EFT N^{2}LO *NNN* interaction. The regulator function was chosen in a form consistent with that used in [11] and [13]: $F(q^2;\Lambda) = \exp[-q^4/\Lambda^4]$ (11). We note that the momentum-space N^{3}LO *NN* interaction is regulated with the nucleon momentum cutoff, while our local chiral EFT N^{2}LO *NNN* interaction is regulated with the momentum transfer cutoff. Due to the choice of the fourth power of the momentum (11), this inconsistency is beyond the order at which our calculations are performed. Values of the c_D and c_E LECs are constrained by a fit to the $A = 3$ system binding energy [18, 14]. Obviously, additional constraints are needed to uniquely determine values of c_D and c_E, see [11, 18, 14, 39] for discussions of different possibilities. Here we are interested only in convergence properties of our

Table 1 *NNN* interaction parameters used in the present calculations. The regulator function was chosen in the form $F(q^2;\Lambda) = \exp[-q^4/\Lambda^4]$

c_1 [GeV^{-1}]	c_3 [GeV^{-1}]	c_4 [GeV^{-1}]	c_D	c_E
−0.81	−3.2	5.4	1.0	−0.029
Λ [MeV]	Λ_χ [MeV]	M_π [MeV]	g_A	F_π [MeV]
500	700	138	1.29	92.4

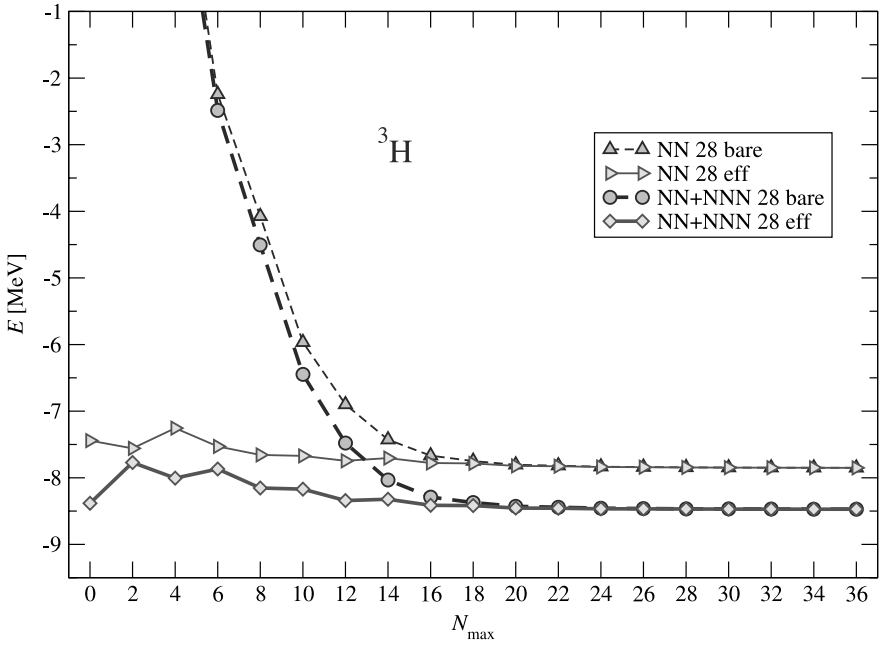

Fig. 6 ^{3}H ground-state energy dependence on the size of the basis. The HO frequency of $\hbar\Omega = 28$ MeV was employed. Results with (thick lines) and without (thin lines) the *NNN* interaction are shown. The full lines correspond to calculations with two-body effective interaction derived from the chiral *NN* interaction, the dashed lines to calculations with the bare chiral *NN* interaction. For further details see the text

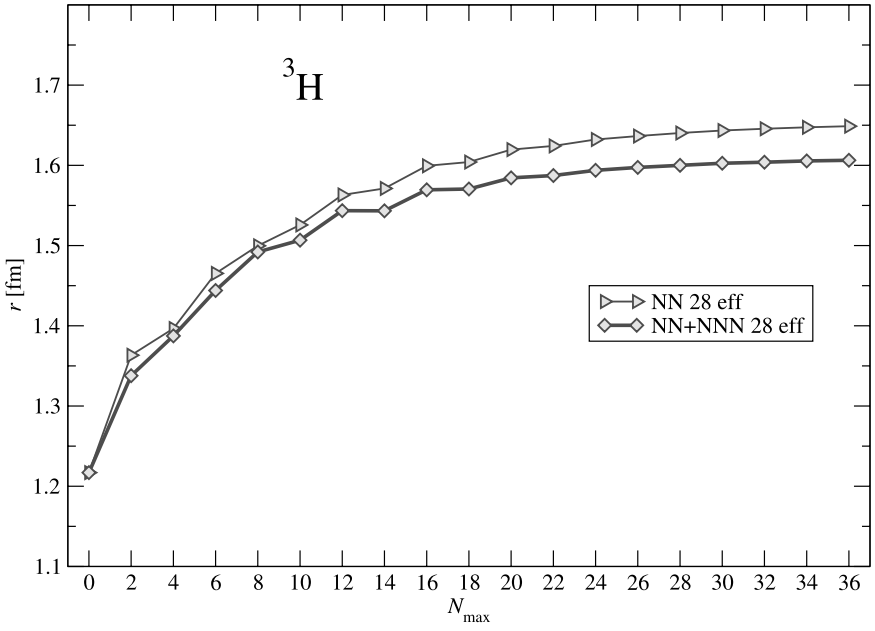

Fig. 7 ^{3}H point-proton rms radius dependence on the size of the basis. The HO frequency of $\hbar\Omega = 28$ MeV was employed. Results with (thick line) and without (thin line) the *NNN* interaction are shown. The two-body effective interaction derived from the chiral *NN* interaction was used in the calculation. For further details see the text

calculations. Therefore, we simply select a reasonable value, e.g., $c_D = 1$, and follow [14] and adopt the c_E value as an average of fits to ^{3}H and ^{3}He binding energies. In Table 1, we summarize the *NNN* interaction parameters used in calculations described in this section. We note that ^{4}He results obtained with the identical Hamiltonian but with $c_D = -1$ and $c_E = -0.331$ are presented in [17].

We use the Jacobi coordinate HO basis antisymmetrized according to the method described in [35]. In Figs. 6 and 7, we show the convergence of the ^{3}H ground-state energy and point-proton rms radius, respectively, with the size of the basis. Thin lines correspond to results obtained with the *NN* interaction only. Thick lines correspond to calculations that also include the *NNN* interaction. The full lines correspond to calculations with two-body effective interaction derived from the chiral EFT N^{3}LO *NN* interaction. The procedure for the effective interaction derivation is described, e.g., in [15, 35]. The dashed lines correspond to calculations with the bare chiral EFT N^{3}LO *NN* interaction. Here, the bare means the original *NN* interaction not renormalized by the effective interaction procedure. The bare *NNN* interaction is added to either the bare *NN* or to the effective *NN* interaction in calculations depicted by thick lines. We observe that the convergence is faster when the two-body effective interaction is used. However, starting at about $N_{\max} = 24$ the convergence is reached also in calculations with the bare *NN* interaction. The rate of convergence also depends on the choice of the HO frequency. In general, it is always advantageous to use the effective interaction in order to improve the convergence rate. The ^{3}H ground-state energy and point-proton radius results are summarized in Table 2. The contributions of different *NNN* terms to the ^{3}H ground-state energy are presented in Table 3. In addition to results obtained using

Table 2 Ground-state energy and point-proton rms radius of ^{3}H and ^{4}He calculated using the chiral N^{3}LO *NN* potential [13] with and without the local chiral N^{2}LO *NNN* interaction. The LEC values and other parameters are given in Table 1. The calculations were performed within the *ab initio* NCSM

	^{3}H		
	NN	*NN* + *NNN*	Expt.
E_{gs} [MeV]	−7.852(5)	−8.473(5)	−8.482
r_p [fm]	1.650(5)	1.608(5)	
	^{4}He		
	NN	*NN* + *NNN*	Expt.
E_{gs} [MeV]	−25.39(1)	−28.34(2)	−28.296
r_p [fm]	1.515(2)	1.475(2)	1.455(7)

Table 3 Contributions of different *NNN* terms to the ^{3}H ground-state energy. The c_D and c_E LECs are explicitly shown. Other parameters are given in Table 1. All energies are given in MeV. The two alternative one-pion-exchange plus contact terms (28) and (29) are considered

^{3}H					
c_D	c_E	E_{gs}	*c* terms	*D* term	*E* term
1.0 (Eq. (28))	−0.029	−8.473	−1.01	0.13	0.03
−1.0 (Eq. (28))	−0.331	−8.474	−1.07	−0.16	0.32
1.0 (Eq. (29))	−0.159	−8.471	−0.99	0.005	0.14
−1.0 (Eq. (29))	−0.213	−8.474	−1.10	−0.05	0.21

the $c_D = 1$, we also show in Table 3 results obtained using $c_D = -1$ and a corresponding c_E constrained by the average of the ^{3}H and ^{3}He binding energy fit. For completeness, we show results obtained by the two alternative one-pion-exchange plus contact terms (28) and (29). In all cases, the contact *E*-term gives a positive contribution. The contribution from the *D*-term changes sign depending on the choice of c_D. Still, the two-pion exchange *c*-terms dominate the *NNN* expectation value.

In Figs. 8 and 9, we show convergence of the ^{4}He ground-state energy and point-proton rms radius, respectively. The NCSM calculations are performed in basis spaces up to $N_{max} = 20$. Thin lines correspond to results obtained with the *NN* interaction only, while thick lines correspond to calculations that also include the *NNN* interaction. The dashed lines correspond to results obtained with bare interactions. The full lines correspond to results obtained using three-body effective interaction (the NCSM three-body cluster approximation, see, e.g., [16, 35]). It is apparent that the use of the three-body effective interaction improves the convergence rate dramatically. We can see that at about $N_{max} = 18$ the bare interaction calculation reaches convergence as well. It should be noted, however, that *p*-shell calculations with the *NNN* interactions are presently feasible in model spaces up to $N_{max} = 6$ or $N_{max} = 8$. The use of the three-body effective interaction is then essential in the *p*-shell calculations.

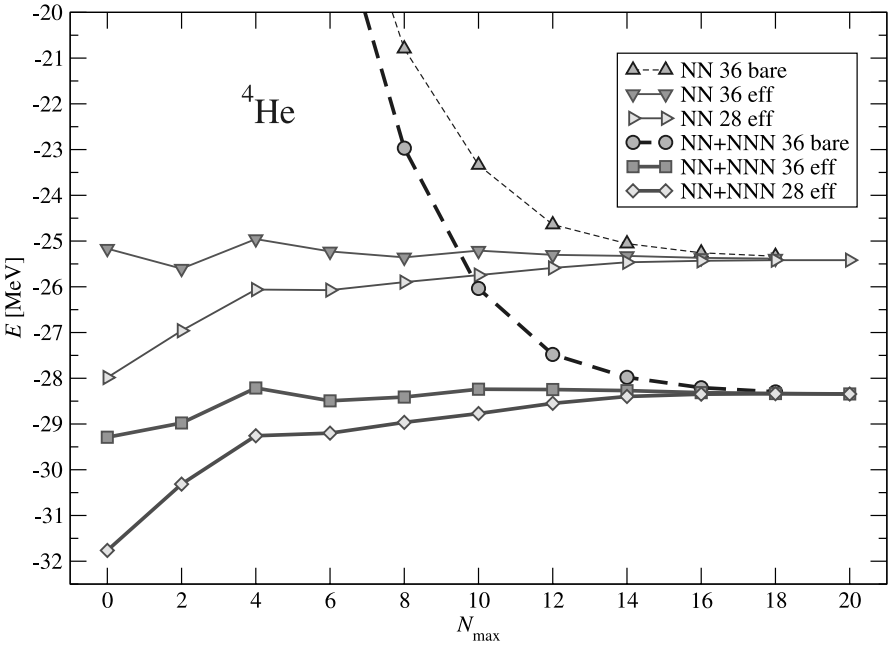

Fig. 8 ^{4}He ground-state energy dependence on the size of the basis. The HO frequencies of $\hbar\Omega = 28$ and 36 MeV were employed. Results with (thick lines) and without (thin lines) the *NNN* interaction are shown. The full lines correspond to calculations with three-body effective interaction, the dashed lines to calculations with the bare interaction. For further details see the text

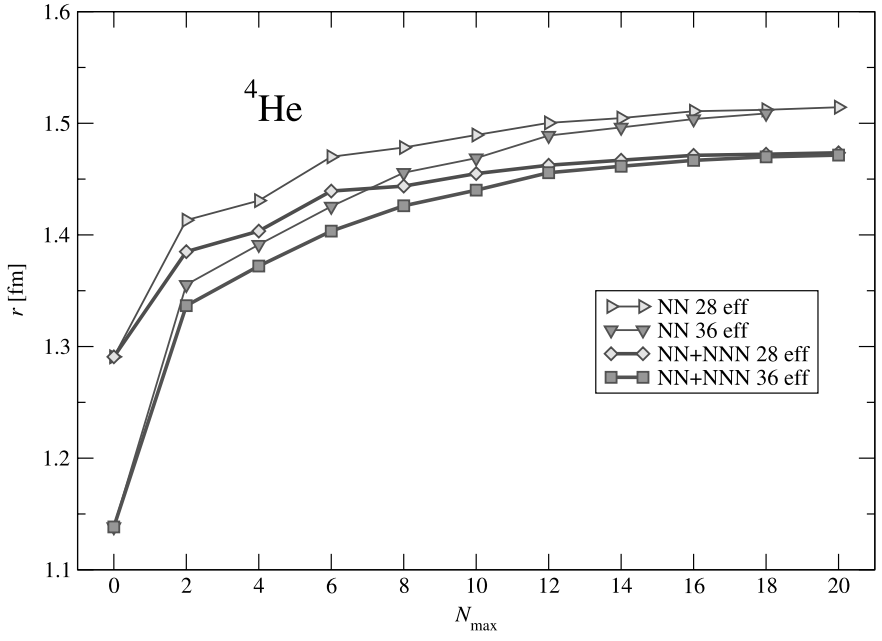

Fig. 9 ^{4}He point-proton rms radius dependence on the size of the basis. The HO frequencies of $\hbar\Omega = 28$ and 36 MeV were employed. Results with (thick line) and without (thin line) the *NNN* interaction are shown. The three-body effective interaction was used in the calculation. For further details see the text

We note that NCSM calculations in the three-body cluster approximation are rather involved. The ^{4}He NCSM calculation with the three-body effective interaction proceeds in three steps. First, we diagonalize the Hamiltonian with and without the *NNN* interaction in a three-nucleon basis for all relevant three-body channels. In the second step, we use the three-body solutions from the first step to derive three-body effective interactions with and without the *NNN* interaction. By subtracting the two effective interactions we isolate the *NN* and *NNN* contributions. This is needed due to a different scaling with particle number of the two- and the three-body interactions. The ^{4}He effective interaction is then obtained by adding the two contributions with the appropriate scaling factors [16]. In the third step, we diagonalize the resulting Hamiltonian in the antisymmetrized four-nucleon Jacobi-coordinate HO basis to obtain the ^{4}He $J^\pi T = 0^+0$ ground state. Obviously, in calculations without the *NNN* interaction, the above three steps are simplified as no *NNN* contribution needs to be isolated. In addition, in the case of no *NNN* interaction, we may use just the two-body effective interaction (two-body cluster approximation), which is much simpler. The convergence is slower, however, see discussion in [40]. We also note that ^{4}He properties with the chiral N^{3}LO *NN* interaction that we employ here were calculated using the two-body cluster approximation in [41] and the present results are in agreement with results found there.

Our ^{4}He results are summarized in Table 2. We note that the present NCSM ^{3}H and ^{4}He results obtained with the chiral N^{3}LO *NN* interaction are in a perfect agreement with results obtained using the variational calculations in the hyperspherical harmonics basis as well as with the Faddeev-Yakubovsky calculations published in [42]. A satisfying feature of the present NCSM calculation is the fact that the rate of convergence is not affected in any significant way by inclusion of the *NNN* interaction.

4 Conclusions

In this paper, we regulated the *NNN* interaction derived within the chiral effective field theory at the N^{2}LO with a function depending on the magnitude of the momentum transfer. The regulated *NNN* interaction is local in coordinate space. This is advantageous for some many-body techniques. In addition, it was found that this interaction performs slightly better in mid-*p*-shell nuclei than its nonlocal counterpart [14, 38]. We calculated matrix elements of the local chiral *NNN* interaction in the three-nucleon HO basis and performed calculations for ^{3}H and ^{4}He within the *ab initio* NCSM. We demonstrated that a very good convergence of the ground-state properties of these nuclei remains unchanged when the *NNN* interaction is added to the Hamiltonian. Expressions for the local χEFT *NNN* interaction matrix elements derived in this paper may by used after some modifications with other bases, e.g., with the hyperspherical harmonics basis.

Acknowledgement I would like to thank U. van Kolck, E. Epelbaum and J. Adam, Jr. for useful comments and A. Nogga for code benchmarking. This work performed under the auspices of the U.S. Department of Energy by Lawrence Livermore National Laboratory under Contract DE-AC52-07NA27344. Support from the LDRD contract No. 04–ERD–058 and from U.S. DOE/SC/NP (Work Proposal Number SCW0498) is acknowledged. This work was also supported in part by the Department of Energy under Grant DE-FC02-07ER41457.

References

1. Weinberg S (1979) Physica 96A:327; (1990) Phys Lett B 251:288; (1991) Nucl Phys B 363:3; Gasser J, et al. (1984) Ann of Phys 158:142; (1985) Nucl Phys B 250:465
2. Bernard V, Kaiser N, Meißner U-G (1995) Int J Mod Phys E 4:193
3. Ordonez C, Ray L, van Kolck U (1994) Phys Rev Lett 72:1982; (1996) Phys Rev C 53:2086
4. van Kolck U (1999) Prog Part Nucl Phys 43:337
5. Bedaque PF, van Kolck U (2002) Ann Rev Nucl Part Sci 52:339; Epelbaum E (2006) Prog Part Nucl Phys 57:654
6. Beane SR, Bedaque PF, Orginos K, Savage MJ (2006) Phys Rev Lett 97:012001
7. Beane SR, Bedaque PF, Savage MJ, van Kolck U (2002) Nucl Phys A 700:377; Nogga A, Timmermans RG, van Kolck U (2005) Phys Rev C 72:054006
8. Birse MC (2006) Phys Rev C 74:014003
9. Epelbaum E, Meißner U-G [nucl-th/0609037]
10. van Kolck U (1994) Phys Rev C 49:2932
11. Epelbaum E, Nogga A, Glöckle W, Kamada H, Meißner U-G, Witała H (2002) Phys Rev C 66:064001
12. Epelbaum E (2006) Phys Lett B 639:456
13. Entem DR, Machleidt R (2003) Phys Rev C 68:041001(R)
14. Navrátil P, Gueorguiev VG, Vary JP, Ormand WE, Nogga A (2007) Phys Rev Lett 99:042501; [nucl-th/0701038]
15. Navrátil P, Vary JP, Barrett BR (2000) Phys Rev Lett 84:5728; (2000) Phys Rev C 62:054311
16. Navrátil P, Ormand WE (2003) Phys Rev C 68:034305
17. Quaglioni S, Navrátil P (2007) Phys Lett B 652:370
18. Nogga A, Navrátil P, Barrett BR, Vary JP (2006) Phys Rev C 73:064002
19. Pudliner BS, Pandharipande VR, Carlson J, Wiringa RB (1995) Phys Rev Lett 74:4396
20. Coon SA, Scadron MD, McNamee PC, Barrett BR, Blatt DWE, McKellar BHJ (1979) Nucl Phys A 317:242
21. Friar JL, Hüber D, van Kolck U (1999) Phys Rev C 59:53
22. Coon SA, Han HK (2001) Few Body Syst 30:131
23. Pieper SC (2005) Nucl Phys A 571:516
24. Pieper SC, Wiringa RB, Carlson J (2004) Phys Rev C 70:054325
25. Wiringa RB, Stoks VGJ, Schiavilla R (1995) Phys Rev C 51:38
26. Pieper SC, Pandharipande VR, Wiringa RB, Carlson J (2001) Phys Rev C 64:014001
27. Pieper SC, Varga K, Wiringa RB (2002) Phys Rev C 66:044310; Wiringa RB, Pieper SC (2002) Phys Rev Lett 89:182501
28. Coon SA, Glöckle W (1981) Phys Rev C 23:1790
29. Friar JL, Gibson BF, Payne GL, Coon SA (1988) Few Body Syst 5:13
30. Coon SA, Peña MT (1993) Phys Rev C 48:2559
31. Hüber D, Witała H, Nogga A, Glöckle W, Kamada H (1997) Few Body Syst 22:107
32. Hüber D, Friar JL, Nogga A, Witała H, van Kolck U (2001) Few Body Syst 30:95
33. Barnea N, Efros VD, Leidemann W, Orlandini G (2004) Few Body Syst 35:155
34. Adam J Jr, Peña MT, Stadler A (2004) Phys Rev C 69:034008
35. Navrátil P, Kamuntavičius GP, Barrett BR (2000) Phys Rev C 61:044001
36. Machleidt R, Holinde K, Elster Ch (1987) Phys Rep 149:1
37. Marsden DCJ, Navrátil P, Coon SA, Barrett BR (2002) Phys Rev C 66:044007
38. Nogga A (private communication)
39. Hanhart C, van Kolck U, Miller GA (2000) Phys Rev Lett 85:2905
40. Navrátil P, Ormand WE (2002) Phys Rev Lett 88:152502
41. Navrátil P, Caurier E (2004) Phys Rev C 69:014311
42. Viviani M, Marcucci LE, Rosati S, Kievsky A, Girlanda L (2006) Few Body Syst 39:159